Chemical Engineering Journal 151 (2009) 122–133

Contents lists available at ScienceDirect

Chemical Engineering Journal

journal homepage: www.elsevier.com/locate/cej

# Novel model development for sorption of arsenate on chitosan

Katrina C.M. Kwok[a], Vinci K.C. Lee[a], Claire Gerente[b], Gordon McKay[a,*]

[a] Department of Chemical Engineering, Hong Kong University of Science and Technology, Clear Water Bay, Kowloon, Hong Kong
[b] Département Systèmes Energétiques et Environnement, École des Mines de Nantes, 4, rue Alfred Kastler, B.P. 20722, F-44307 Nantes Cedex 3, France

ARTICLE INFO

*Article history:*
Received 22 June 2008
Received in revised form 31 January 2009
Accepted 10 February 2009

*Keywords:*
Equilibrium
Kinetics
Modelling
Arsenate
Chitosan

ABSTRACT

The sorption of arsenate onto chitosan flakes has been studied. Chitosan, a natural, non-toxic, biodegradable polysaccharide is derived by the deacetylation of chitin, a major component of crustacean shells of prawn, crab or shrimp. Its main attributes correspond to its polycationic nature and the abundance of amine functional groups. Chitosans have received increasing attention as renewable polymeric materials for the treatment of metal contaminated water and wastewater.

The effect of initial pH on the sorption isotherm has been studied for two initial concentration ranges of arsenate (0–3000 $\mu g\,L^{-1}$ and 0–10,000 $\mu g\,L^{-1}$) on chitosan. The equilibrium data have been modelled using Langmuir and Freundlich type isotherms at three initial pH values. The maximum adsorption capacity occurs at an initial pH 3.5 and empirical correlations have been developed to model the effect of pH on the sorption isotherm parameters. Each initial $pH_i$ value, namely, 3.5, 4.0 and 4.5, corresponded to a fixed final $pH_e$ value, namely, 4.69, 6.40 and 6.73 respectively.

A series of batch kinetic experiments has been carried out at different initial pH values. The arsenate sorption process appears to be completed after 30 min, however, a previously unreported phenomenon was observed, namely, a steady desorption of arsenate.

There is a natural buffering effect from the chitosan. The batch kinetic data have been correlated using the pseudo-first order, pseudo-second order and pseudo-first order reversible models; this latter model was modified to incorporate the arsenate desorption step as a function of the changing system pH.



## 1. Introduction

Arsenic, as arsenites As(III) and arsenates As(V), contamination of natural waters is a serious problem in several countries. The concentrations of arsenic in groundwater and surface waters are higher than allowed levels raising health concerns in many parts of the world, including Taiwan, Vietnam [1,2] and the western United States [3].

Arsenic is known as a poison of acute toxicity and has long-term carcinogenic properties, particularly with respect to lung and skin cancer [4]. The European Commission (EC, 1998) [5], the US Environmental Protection Agency [6] and the World Health Organization (WHO) [7] have all recently revised the maximum concentration limit for arsenic in drinking water by decreasing it from 50 $\mu g\,L^{-1}$ to 10 $\mu g\,L^{-1}$.

Consequently, it is a major issue to develop effective treatment methods for the removal of arsenic from drinking waters to reach this limit. Due to the two species of arsenic, this enhances the treatment problem. Conventional technologies include coagulation, precipitation, and coprecipitation with iron and aluminum compounds [8]. Sorption onto a range of materials including alumina and active carbons [9], ion exchange and membrane technologies has been investigated [10]. As(V) is better removed than As(III) but this latter is problematic unless it can be oxidized to the As(V) form. Most research has focused on the addition of iron compounds and oxidation technologies [11]. Goethite and hematite have been widely used for the sorption of As(III) and As(V) [12]. Arsenic sorption on ferrihydrite [13] and amorphous iron oxide [14,15] has been studied.

In the present study the sorption of arsenate ions onto a low cost biosorbent, chitosan [16] has been studied over a range of initial pH values ($pH_i$). The equilibrium isotherms have been determined and analyzed by developing the correlations of sorption capacity versus initial pH ($pH_i$) and equilibrium pH ($pH_e$). Furthermore, a series of batch kinetic studies have been performed and modelled using a reversible first order kinetic equation. The variation of pH in the kinetic studies was correlated with the contact time of the adsorbate and adsorbents, providing the information on the pH profile throughout the reaction. In addition, an empirical equation has been developed to correlate the rate constants of adsorption and desorption with pH value of the reaction.

* Corresponding author. Tel.: +852 2358 8412; fax: +852 2358 0054.
*E-mail address:* kemckayg@ust.hk (G. McKay).

1385-8947/$ – see front matter © 2009 Elsevier B.V. All rights reserved.
doi:10.1016/j.cej.2009.02.004

**Nomenclature**

| | |
|---|---|
| $a_L$ | Langmuir isotherm constant (L/μg) |
| $\alpha_{K,j}^{(a)}$ | empirical parameter of initial $pH_i$ in Correlation A in Eq. (7) |
| $\alpha_{a,j}^{(a)}$ | empirical parameter of initial $pH_i$ in Correlation A in Eq. (8) |
| $\alpha_{K,j}^{(b)}$ | empirical parameter of initial $pH_i$ in Correlation B in Eq. (9) |
| $\alpha_{a,j}^{(b)}$ | empirical parameter of initial $pH_i$ in Correlation B in Eq. (10) |
| $\alpha_{K,j}^{(c)}$ | empirical minimum value of initial $pH_i$ in Correlation C in Eq. (11) |
| $\alpha_{a,j}^{(c)}$ | empirical minimum value of initial $pH_i$ in Correlation C in Eq. (12) |
| $b_F$ | Freundlich isotherm constant (dimensionless) |
| $\beta_{K,j}^{(a)}$ | exponent parameter of initial $pH_i$ in Correlation A in Eq. (7) |
| $\beta_{a,j}^{(a)}$ | exponent parameter of initial $pH_i$ in Correlation A in Eq. (8) |
| $\beta_{K,j}^{(b)}$ | empirical parameter of initial $pH_i$ in Correlation B in Eq. (9) |
| $\beta_{a,j}^{(b)}$ | empirical parameter of initial $pH_i$ in Correlation B in Eq. (10) |
| $\beta_{K,j}^{(c)}$ | empirical minimum value of $K_j$ for isotherm $j$ in Correlation C in Eq. (11) |
| $\beta_{a,j}^{(c)}$ | empirical minimum value of $a_j$ for isotherm $j$ in Correlation C in Eq. (12) |
| $c_F$ | $y$-intercept of initial pH correlation to $b_j$ for isotherm $j$ (Eq. (13)) |
| $C_0$ | initial liquid-phase concentration ($\mu g\,L^{-1}$) |
| $C_e$ | equilibrium liquid-phase concentration ($\mu g\,L^{-1}$) |
| $\gamma_{K,J}^{(c)}$ | empirical inverse proportional parameter in Eq. (11) |
| $\gamma_{a,J}^{(c)}$ | empirical inverse proportional parameter in Eq. (12) |
| $K_L$ | Langmuir isotherm constant ($L/g^{-1}$) |
| $K_F$ | Freundlich isotherm constant $((l)^{b_F}(\mu g)^{1-b_F}/g)$ |
| $k_{+1}$ | rate constant of sorption in Eq. (16) |
| $k_{-1}$ | rate constant of desorption in Eq. (17) |
| $m_F$ | slope of initial pH correlation to $b_j$ for isotherm $j$ (Eq. (13)) |
| $pH_i$ | initial pH |
| $pH_e$ | equilibrium pH |
| $q_e$ | equilibrium solid-phase concentration (μg/g) |
| $q_{max}$ | maximum sorption capacity (μg/g) |
| $q_t$ | solid-phase concentration at time $t$ (μg/g) |
| SSE | sum of the squares of the error (dimensionless, nonlinear regressive method) |

## 2. Materials and methods

### 2.1. Chitosan

Chitosan (poly-β(1-4)-2-amino-2-deoxy-D-glucose) is a partially deacetylated polymer of acetylglucosamine [17], and it is prepared from chitin (poly-β(1-4)-2-acetamido-2-deoxy-D-glucose). The chitosan flakes used in this research were purchased from Sigma Chemical Company as a practical grade material extracted from crab shells with minimum 85% degree of deacetylation.

### 2.2. Pretreatment of chitosan

The commercial chitosan was sieved into discrete particle size ranges (250–355 μm) with stainless steel sieves (BS410/1986, Endecotts Ltd.). The portion was rinsed several times with deionised water to desorb any impurities and was dried under vacuum for three days and kept in a dessicator before use. The properties of chitosan, including its density, porosity, specific surface area and its surface charge in terms of the point of zero charge ($pH_{pzc}$) were characterized and the data are shown in Table 1.

### 2.3. Sodium arsenate and determination

All chemicals were reagent grade and they were used without further purification. All solutions were prepared with deionised water. A stock solution of As(V) was prepared from the dissolution of sodium arsenate heptahydrate salt ($Na_2HAsO_4{\bullet}7H_2O$) (Aldrich Chemical Company, Inc.) at a concentration of 500 mg $L^{-1}$.

Hydride generation inductively coupled argon plasma optical emission spectroscopic analysis (HY-OES-ICP) using a continuous flow system (PerkinElmer OPTIMA 3000 XL) was used to measure the concentration of arsenic in water. Hydride generation techniques have been combined with ICP optical emission spectrometry (ICP-OES) for the routine determination of concentration of arsenic since 1978.

### 2.4. Equilibrium studies

To determine the equilibrium isotherms, a series of As(V) solutions with initial concentration ranged between 250 μg $L^{-1}$ and 10,000 μg $L^{-1}$ were prepared by diluting a 500 mg $L^{-1}$ stock solution with deionised water. The pH values of the As(V) solutions were initially adjusted to the range from pH 3.50 ± 0.05 to pH 5.50 ± 0.05 by addition of 0.1 M hydrochloric acid and were measured with a digital pH meter (Orion, model 420A pH meter). The temperature was maintained at 24 ± 2 °C and 0.0250 g of commercial chitosan, with particle size range of 250–355 μm, was agitated with 50 mL of aqueous As(V) solution in a capped 125-ml HDPE bottles with an orbital shaker (Heidolph UNIMAX 1010 and Heidolph INKUBATOR 1000) at 200 rpm for 96 h. This contact time allows the dispersion of chitosan and arsenate solution to reach equilibrium, as determined during preliminary experiments. Each tested suspension was collected after sufficient settling time of 2 min, and then the upper clear solution was collected for measuring of residual As(V) concentration. The equilibrium pH values of the aqueous phase were also determined.

### 2.5. Batch kinetic experiments

The sorption kinetic studies of As(V) on chitosan were evaluated by agitating 0.850 g of chitosan with particle size range of 250–355 μm in 1.7 L of aqueous As(V) solution for 6 h in the batch kinetic system. The volume-to-mass ratio of As(V) solution and chitosan was kept the same as in the equilibrium studies. The impeller speed was calibrated to 400 rpm with the optical tachometers (Cole-Parmer 87303-10 series). The temperature was maintained at 24 ± 2 °C. The pH of the As(V) solution with the concentration of 3000 μg $L^{-1}$ was initially adjusted to the range from $pH_i$ 3.50 ± 0.05 to $pH_i$ 5.50 ± 0.05, the same as in the equilibrium studies. The concentration of the As(V) solution at different time intervals in the process was analyzed. The results were plotted as $C_t/C_0$ versus time (min). The pH values of the aqueous phase were determined simultaneously and were plotted against contact time.

**Table 1**
Characterizations of chitosan used in present study.

| Particle size of chitosan (μm) | Surface area ($m^2\ g^{-1}$) | Total pore volume ($cm^3\ g^{-1}$) | Average density ($g\ cm^{-3}$) | $pH_{pzc}$ |
|---|---|---|---|---|
| 250–355 | 1.1190 | 2.688E−02 | 1.4688 | 9.0345 |
| 355–500 | 0.7258 | 1.931E−02 | 1.4757 | 8.6034 |
| 500–710 | 0.0586 | 9.138E−03 | 1.4978 | 8.4784 |
| 710–1000 | 0.2981 | 1.943E−02 | 1.4787 | 8.3017 |

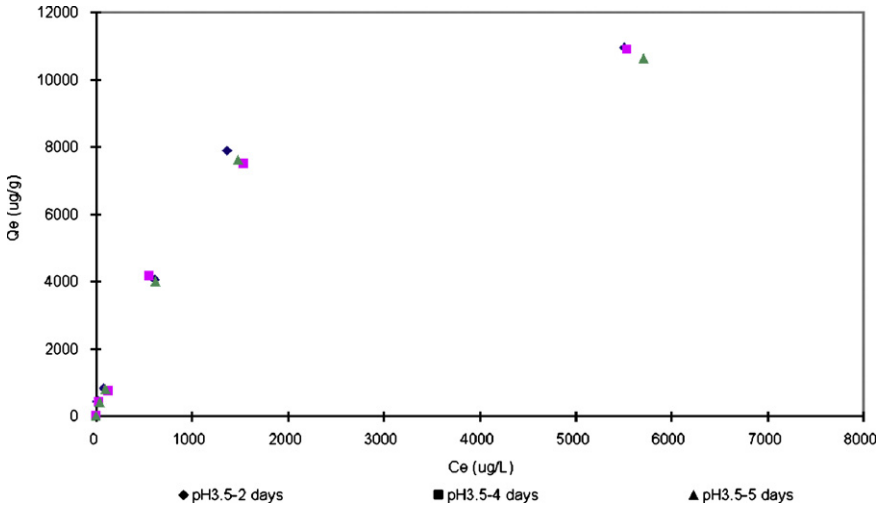


**Fig. 1.** The equilibrium contact time studies of arsenate ions on chitosan.

## 3. Results and discussion

Sorption isotherms describe how adsorbates interact with adsorbents and so are critical in optimising the use of adsorbents. Therefore, the correlation of equilibrium data either by theoretical or by empirical equations is essential to the practical design and operation of attracting and concentrating a solute from solution onto its surface. The rate and capacity of this process depends on the chemical nature of both solute and adsorbent and the physical process design of the contacting system. Several factors are known to influence the time required for a sorbate–sorbent system reach equilibrium and the main ones are: sorbate–sorbent affinity, extent of the system agitation, mechanism of sorption (reaction, diffusion and ion exchange), solution pH, concentration of solute and sorbent, presence of other dissolved species, sorbent particle size and solution temperature.

The time required for an arsenate–adsorbent system to reach equilibrium must be determined in order to establish the validity of the experimental equilibrium studies data prior to determining the isotherm equation.

### 3.1. Factors affecting equilibrium contact time

The results in Fig. 1 show that for five different initial arsenate concentrations, the times to reach equilibrium are 48 h or less for all initial arsenate concentrations from 250 $\mu g\ L^{-1}$ to 10,000 $\mu g\ L^{-1}$. The results for initial arsenate concentrations of 250 $\mu g\ L^{-1}$, 500 $\mu g\ L^{-1}$, 2500 $\mu g\ L^{-1}$, 5000 $\mu g\ L^{-1}$ and 10,000 $\mu g\ L^{-1}$ are shown in Fig. 1 at initial pH value of 3.50. On this basis, all equilibrium studies in the present work would use a safe contact time of 96 h to ensure equilibrium has been achieved over the whole concentration spectrum.

### 3.2. Analysis of equilibrium isotherms

Consequently, to effect adsorber design, it is necessary to establish the most accurate correlation of the equilibrium data by means of an isotherm equation model. There are several well-established correlations in the literature, the two main ones are:

- Langmuir [18] and
- Freundlich [19].

The application of the range of isotherms for the sorption of both arsenate and arsenite on adsorbents has been very limited in the literature to 3 (or 4) isotherms only, namely, Langmuir, Freundlich, Dubinin–Radushkevich and the linear isotherm. The Langmuir and Freundlich isotherms will be discussed in detail in the present study, and will be applied in the present studies. The Redlich–Peterson incorporates features of both the Langmuir and

**Table 2**
Langmuir isotherm constants and the monolayer capacities at different $pH_i$ and $pH_e$ values in adsorption of arsenate on chitosan.

| $pH_i$ | $pH_e$ | $a_L$ | $K_L$ | $K_L/a_L$ | SSE |
|---|---|---|---|---|---|
| 3.5 | 4.69 | 6.56E−04 | 9.29E+00 | 14162.80 | 1.01E+06 |
| 3.6 | 5.27 | 2.35E−04 | 3.39E+00 | 14413.06 | 1.38E+06 |
| 3.7 | 5.60 | 1.42E−04 | 2.14E+00 | 15060.15 | 8.04E+05 |
| 4.0 | 6.40 | 1.39E−04 | 8.81E−01 | 6352.01 | 1.75E+05 |
| 4.3 | 6.60 | 9.00E−05 | 4.41E−01 | 4905.28 | 2.51E+05 |
| 4.6 | 6.73 | 8.39E−05 | 2.21E−01 | 2630.90 | 3.82E+04 |
| 5.0 | 6.84 | 8.33E−05 | 2.08E−01 | 2496.13 | 5.18E+04 |
| 5.5 | 6.95 | 8.25E−05 | 1.10E−01 | 1330.83 | 2.49E+04 |

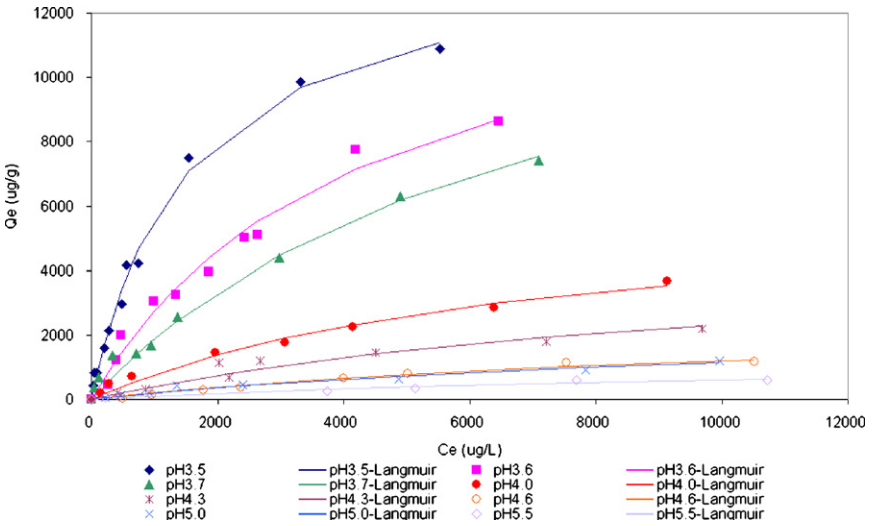


**Fig. 2.** Equilibrium studies and Langmuir isotherm of arsenate ions on chitosan.

**Table 3**
Langmuir parameters and sorption capacities from the literature.

| Adsorbent | As form | Conditions | | | Constants | | | Ref. |
|---|---|---|---|---|---|---|---|---|
| | | pH | $T$ (°C) | Co (max) (mg $L^{-1}$) | $K_L$ (L $mg^{-1}$) | $a_L$ (L $mg^{-1}$) | $q_m$ (mg $g^{-1}$) | |
| Hematite | As(V) | 4.2 | 20 | 9.965E+00 | 1.580E−03 | 7.210E+00 | 2.190E−01 | [15] |
| Hematite | As(V) | 4.2 | 30 | 9.965E+00 | 1.070E−03 | 5.220E+00 | 2.050E−01 | |
| Hematite | As(V) | 4.2 | 40 | 9.965E+00 | 8.630E−04 | 4.640E+00 | 1.860E−01 | |
| Feldspar | As(V) | 6.2 | 20 | 9.965E+00 | 8.810E−04 | 4.240E+00 | 2.080E−01 | |
| Feldspar | As(V) | 6.2 | 30 | 9.965E+00 | 7.490E−04 | 4.120E+00 | 1.820E−01 | |
| Feldspar | As(V) | 6.2 | 40 | 9.965E+00 | 6.590E−04 | 4.090E+00 | 1.610E−01 | |
| Natural iron ore | As(V) | 5 | 20 | 3.000E+01 | 2.050E−03 | 5.120E+00 | 4.000E−01 | [21] |
| Activated bauxsol | As(V) | 7 | 15 | 1.371E+01 | 1.062E+01 | 5.472E+00 | 1.940E+03 | [28] |
| Activated bauxsol | As(V) | 7 | 20 | 1.019E+01 | 1.503E+01 | 6.941E+00 | 2.165E+03 | |
| Activated bauxsol | As(V) | 7 | 50 | 1.139E+01 | 4.139E+01 | 1.388E+01 | 2.982E+03 | |
| Activated bauxsol | As(V) | 4.5 | 23 | 1.648E+01 | 4.488E+01 | 5.873E+00 | 7.642E+03 | |
| Bauxsol | As(V) | 10 | 23 | 1.199E+01 | 6.080E−02 | 1.335E+00 | 4.555E+02 | |
| Bauxsol | As(V) | 7.5 | 23 | 1.453E+01 | 1.490E+00 | 1.989E+00 | 7.470E+02 | |
| Bauxsol | As(V) | 7.3 | 23 | 2.997E+00 | 2.500E+00 | 3.604E+00 | 6.938E+02 | |
| Bauxsol | As(V) | 6.3 | 23 | 2.397E+00 | 1.097E+01 | 1.014E+01 | 1.081E+03 | |
| Activated bauxsol | As(III) | 6.8 | 23 | 1.176E+01 | 2.310E−01 | 4.271E−01 | 5.409E+02 | |
| Oxisol | As(III) | 5.5 | 25 | – | – | – | 7.500E+00 | [22] |
| Oxisol | As(V) | 5.5 | 25 | – | – | – | 1.240E+01 | |
| Molybdate-chitosan beads (MoCB) | As(V) | 3 | 20 | 2.000E+01 | 2.481E−03 | 2.560E+00 | 9.290E+01 | [35] |
| MoCB-phosphate | As(V) | 3 | 20 | 2.000E+01 | 2.481E−03 | 1.200E+00 | 1.980E+02 | |
| | | | | | L $mg^{-1}$ Mo | L $mg^{-1}$ | | |
| Tropical soil | As(V) | 4.5 | 20 | 7.492E+04 | 9.360E−05 | 4.500E−01 | 2.080E−01 | [36] |
| Fungal biomass | As(V) | 3 | 25 | 1.000E+03 | 1.710E−03 | 7.000E−02 | 2.450E+01 | [27] |
| Modified biomass | As(V) | 3 | 25 | 1.000E+03 | 1.730E−03 | 3.000E−02 | 5.780E+01 | |
| | | | | mg $L^{-1}$ as $Na_2HAsO_4$ | | | | |
| Activated alumina | As(III) | 7.6 | 25 | 1.000E+00 | 1.540E−03 | 8.540E+00 | 1.800E−01 | [12] |
| Activated alumina | As(III) | 7.6 | 35 | 1.000E+00 | 1.200E−03 | 8.280E+00 | 1.450E−01 | |
| Activated alumina | As(III) | 7.6 | 45 | 1.000E+00 | 8.430E−04 | 7.400E+00 | 1.050E−01 | |
| Gibbsite | As(III) | 4 | 25 | 3.746E+00 | 9.877E−01 | 1.922E−02 | 1.461E+00 | [37] |
| Gibbsite | As(III) | 7.5 | 25 | 3.746E+00 | 4.405E−01 | 1.145E−02 | 1.948E+00 | |
| Gibbsite | As(III) | 8.2 | 25 | 3.746E+00 | 1.068E+00 | 3.604E−02 | 2.532E+00 | |
| Akaganeite | As(V) | 7.5 | 25 | 2.000E+01 | 4.365E−01 | 5.850E−02 | 1.341E+02 | [29] |
| Akaganeite | As(V) | 7.5 | 35 | 2.000E+01 | 6.540E−01 | 1.100E−01 | 1.678E+02 | |
| Akaganeite | As(V) | 7.5 | 45 | 2.000E+01 | 1.092E+00 | 2.360E−01 | 2.165E+02 | |
| Quaternised rice husk | As(V) | 7.5 | 28 | 6.000E+02 | – | – | 1.900E+01 | [25] |
| Coconut husk | As(III) | 8.5 | 30 | 4.500E+02 | 3.490E−03 | 2.390E−02 | 1.460E+02 | [26] |
| Coconut husk | As(III) | 8.5 | 50 | 4.500E+02 | 6.710E−03 | 4.360E−02 | 1.540E+02 | |

the Freundlich isotherms and has been included in the data analysis. In classical terms, these isotherms are applied to ideal single component systems [20]. Although these systems, particularly with pH adjustment, contain low levels of other anions in addition to arsenates, the mathematical form of the two isotherms will be used to analyze the experimental equilibrium data.

### 3.2.1. Langmuir type isotherm

The Langmuir sorption isotherm is monolayer adsorption model with the strengths of the intermolecular forces falling off rapidly with distance. The Langmuir isotherm equation [18] and its linear form are shown in Eqs. (1) and (2) respectively:

$$q_e = \frac{K_L C_e}{1 + a_L C_e} \quad (1)$$

$$\frac{C_e}{q_e} = \frac{1}{K_L} + \frac{a_L}{K_L} C_e \quad (2)$$

Whereas, at high sorbate concentrations, the equation predicts a constant monolayer sorption capacity, $q_m$, such that

$$q_m = \frac{K_L}{a_L} \quad (3)$$

The monolayer sorption capacities, $q_m$ and the isotherm constants, $K_L$ and $a_L$, at the different pH values have been determined and are shown in Table 2. The capacities range from 1331 μg arsenate/g chitosan at initial pH ($pH_i$) 5.5 to 14160 μg arsenate/g chitosan at initial pH ($pH_i$) 3.5.

Many studies have been carried out to assess if various adsorbents are feasible to remove arsenate and arsenite from water systems. Most sorption studies, quantified with Langmuir isotherm, are based on iron-containing materials including hematite and feldspar [15], natural iron ores [21], akaganeite nanocrystals, tropical soil-containing significant amounts of iron oxides and oxisol [22]. Another composite of iron and aluminum oxides [23] a waste from aluminum production, known as red mud or bauxsol and its activated form has been widely tested [24]. Wastes such as rice husks [25] and coconut husks [26] which can be readily modified have been studied for arsenic removal. Recent work [27] demonstrates the potential of biosorption for arsenic removal. The sorption results of arsenate anions of various pH values onto chitosan have been analyzed according to the Langmuir type equation and are shown in Fig. 2. The values of the Langmuir parameters for all these studies are presented in Table 3.

Comparing the values of $q_{max}$ achieved by other adsorbents reported in the literature shown in Table 3, with the adsorption capacities of arsenate on chitosan (i.e. the values of $K_L/a_L$), in the present study, shown in Table 2, the chitosan has an adsorption capacity similar to activated bauxsol, bauxsol, [28] and akaganeite [29] in Table 3. The adsorption capacity of chitosan, the biopolymer derivative from waste material, is comparable to the capacities of many of the other adsorbents in Table 3.

### 3.2.2. Freundlich type isotherm

This empirical model can be applied to non-ideal sorption, assuming an exponentially decaying sorption site energy distribution onto heterogeneous surfaces, such as activated carbon, as well as multilayer sorption and is expressed by Eq. (4) and its linear form in Eq. (5):

$$q_e = K_F C_e^{b_F} \quad (4)$$

$$\ln q_e = \ln K_F + b_F \ln C_e \quad (5)$$

In the limits as $b_F$ tends to unity, then the equation approaches Henry's law, that is:

$$q_e = K_F C_e \quad (6)$$

**Table 4**
Freundlich isotherm constants at different $pH_i$ and $pH_e$ values in adsorption of arsenate on chitosan.

| $pH_i$ | $pH_e$ | $K_F$ | $b_F$ | SSE |
|---|---|---|---|---|
| 3.5 | 4.69 | 5.14E+01 | 6.40E−01 | 9.66E+06 |
| 3.6 | 5.27 | 3.33E+01 | 6.40E−01 | 1.77E+06 |
| 3.7 | 5.60 | 2.29E+01 | 6.55E−01 | 5.02E+05 |
| 4.0 | 6.40 | 1.26E+01 | 6.21E−01 | 2.59E+04 |
| 4.3 | 6.60 | 8.35E+00 | 6.08E−01 | 2.20E+05 |
| 4.6 | 6.73 | 3.52E+00 | 6.31E−01 | 9.29E+04 |
| 5.0 | 6.84 | 2.77E+00 | 6.53E−01 | 2.89E+04 |
| 5.5 | 6.95 | 1.61E+00 | 6.43E−01 | 1.95E+04 |

But this limitation is not restricted to low concentrations and consequently the Freundlich equation is still considered as empirical.

The results for the sorption of arsenate anions at various pH values onto chitosan have been analyzed according to the Freundlich equation and are shown in Table 4 and Fig. 3. The Freundlich equation has not been as widely used as the Langmuir equation to analyze arsenic sorption data which usually have a higher correlation coefficient. The arsenate systems studied using the Freundlich isotherm include copper treated activated carbon [30], ruthenium oxide [31], and the sorption of arsenate on ferrihydrite [32].

### 3.3. Development of pH correlations

The comparison of initial pH and equilibrium pH in the isotherm of arsenate and chitosan is shown in Table 5. It is found that the pH value of the aqueous phase increases upon reaction to reach a particular equilibrium pH, which is independent of the initial arsenate concentration, but dependent of the initial pH value. Table 2 demonstrates the variation of isotherm parameters in the present chitosan studies with respect to the change of initial pH, denoted as $pH_i$ and equilibrium pH, namely, $pH_e$. Firstly, the Langmuir isotherm is used as the demonstration of the development of pH correlations. The relationship of the Langmuir isotherm parameters with initial pH ($pH_i$) and equilibrium pH ($pH_e$) are illustrated in Figs. 4–7 respectively. The correlation can be described by the following three types of empirical equations. The pH of the aqueous phase increases from its initial value to an equilibrium value.

Correlation A (power relationship):

$$K_j = \alpha_{K,j}^{(a)} (pH_i)^{-\beta_{K,j}^{(a)}} \quad (7)$$

$$a_j = \alpha_{a,j}^{(a)} (pH_i)^{-\beta_{a,j}^{(a)}} \quad (8)$$

**Table 5**
Comparison of initial pH and equilibrium pH in isotherm of arsenate and chitosan.

| $C_0$ (μg $L^{-1}$) | $C_e$ (μg $L^{-1}$) | $pH_i$ | $pH_e$ |
|---|---|---|---|
| 532 | 86.40 | 3.56 | 4.09 |
| 1,008 | 208.00 | 3.50 | 4.78 |
| 3,036 | 748.00 | 3.54 | 4.51 |
| 5,304 | 1,536.00 | 3.49 | 4.88 |
| 8,250 | 3,320.00 | 3.49 | 4.85 |
| 11,000 | 5,530.00 | 3.49 | 5.04 |
| 521 | 273.00 | 4.00 | 6.18 |
| 1,004 | 646.00 | 4.01 | 6.24 |
| 4,040 | 3,072.00 | 4.05 | 5.45 |
| 3,736 | 4,140.00 | 4.00 | 6.44 |
| 7,810 | 6,380.00 | 3.99 | 6.53 |
| 10,980 | 9,130.00 | 4.00 | 6.49 |
| 507 | 491.00 | 4.59 | 7.07 |
| 1,030 | 964.00 | 4.58 | 6.88 |
| 4,360 | 4,000.00 | 4.62 | 5.79 |
| 5,415 | 5,020.00 | 4.59 | 6.83 |
| 8,110 | 7,535.00 | 4.60 | 7.00 |
| 11,100 | 10,510.00 | 4.59 | 6.83 |

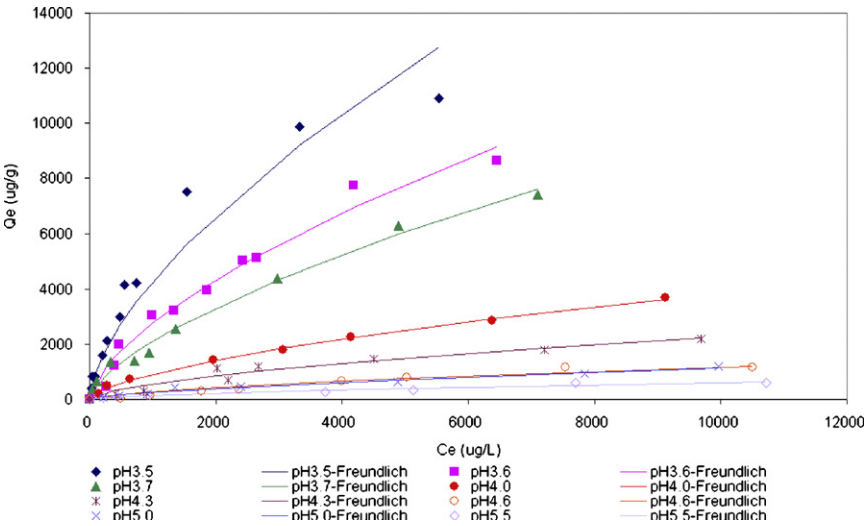


**Fig. 3.** Equilibrium studies and Freundlich isotherm of arsenate ions on chitosan.

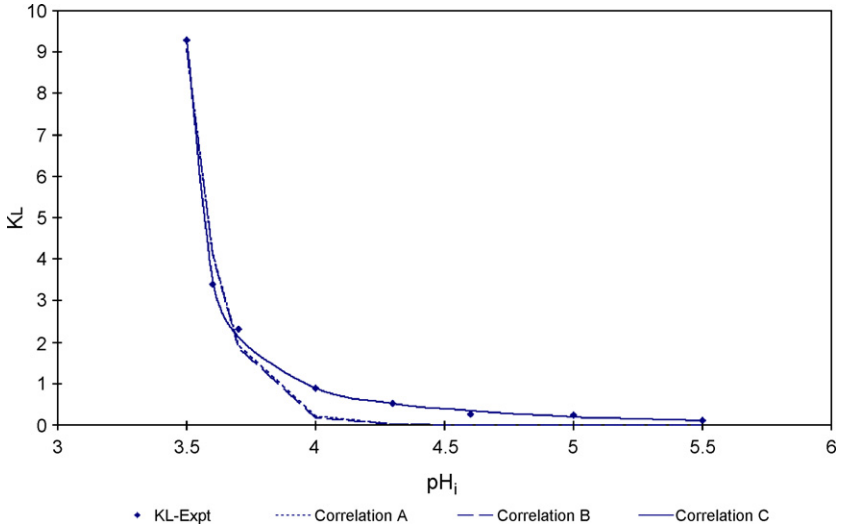


**Fig. 4.** Langmuir isotherm parameter ($K_L$) against initial pH ($pH_i$).

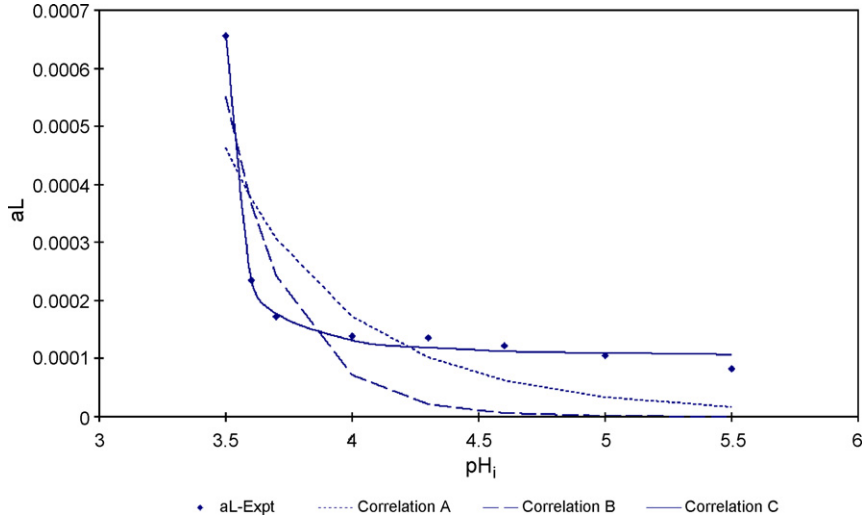


**Fig. 5.** Langmuir isotherm parameter ($a_L$) against initial pH ($pH_i$).

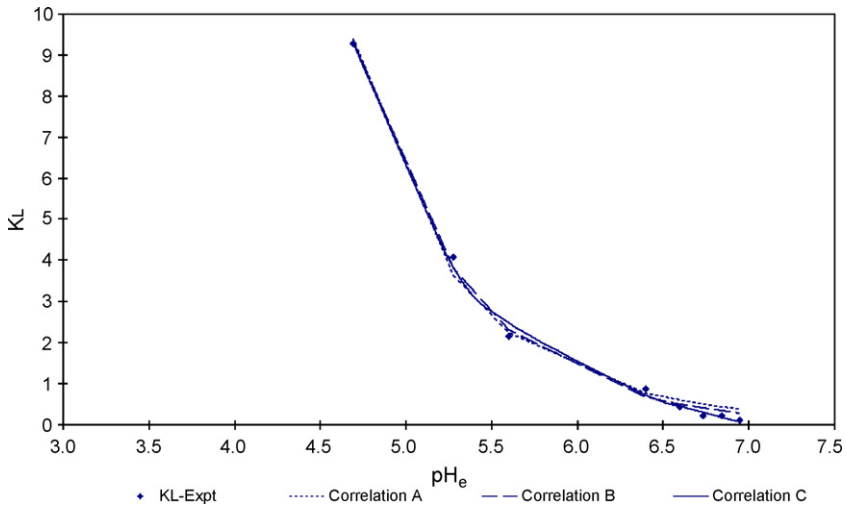


**Fig. 6.** Langmuir isotherm parameter ($K_L$) against equilibrium pH ($pH_e$).

Correlation B (exponent relationship):

$$K_j = \alpha_{K,j}^{(b)} \exp\left(-\beta_{K,j}^{(b)} \times \mathrm{pH}_i\right) \quad (9)$$

$$a_j = \alpha_{a,j}^{(b)} \exp\left(-\beta_{a,j}^{(b)} \times \mathrm{pH}_i\right) \quad (10)$$

Correlation C (inverse proportion relationship):

$$\left(K_j - \beta_{K,j}^{(c)}\right)\left(\mathrm{pH}_i - \alpha_{K,j}^{(c)}\right) = \gamma_{K,j}^{(c)} \quad (11)$$

$$\left(a_j - \beta_{a,j}^{(c)}\right)\left(\mathrm{pH}_i - \alpha_{a,j}^{(c)}\right) = \gamma_{a,j}^{(c)} \quad (12)$$

These empirical correlation parameters with the equilibrium pH values are summarized in Table 6. The mathematical model is constrained by the chemical properties of chitosan and the arsenate ion. For example, chitosan is dissolved at a low pH condition (e.g. pH < 3.0). The concentration of arsenate ion varies with different pH, which is shown in the speciation diagram in Fig. 8. Hence, the empirical equations are only valid to the current experimental range of initial pH and the corresponded fixed equilibrium pH.

Figs. 9 and 10 show the correlation of the Freundlich isotherm parameters ($K_F$ and $b_F$ respectively) with the equilibrium pH ($pH_e$). The correlation of $K_F$ is similar to that of $K_L$ and $a_L$. Hence, the correlation of $K_F$ can also be described by three correlation equations mentioned previously (Eqs. (7), (9) and (11)). The correlation of $b_F$ looks like a linear relationship, which can be modelled by a linear equation:

$$b_F = m_F \mathrm{pH}_i + c_F \quad (13)$$

These empirical correlation parameters ($m_F$ and $c_F$) are summarized in Table 6. The isotherm results modelled by Langmuir type isotherm equation using initial pH, $pH_i$; correlation and equilibrium pH, $pH_e$, correlation are shown in Figs. 11 and 12 respectively.

### 3.4. Selection of optimum pH correlation

There is only one linear correlation of the Freundlich isotherm parameter, $b_F$ (as shown in Eqs. (13)). In the meanwhile, there are three types of empirical correlations for other isotherm parameters, including $K_L$, $a_L$ and $K_F$. The selection of the optimum pH correlation is dependent on the sum of the squared error (SSE), the non-linear regressive method, determined using different pH correlation equations. The sum of the squared error of different pH correlation equations is also shown in Table 6. This table demonstrates that the third correlation, i.e. C (inverse proportion, as shown in Eqs.

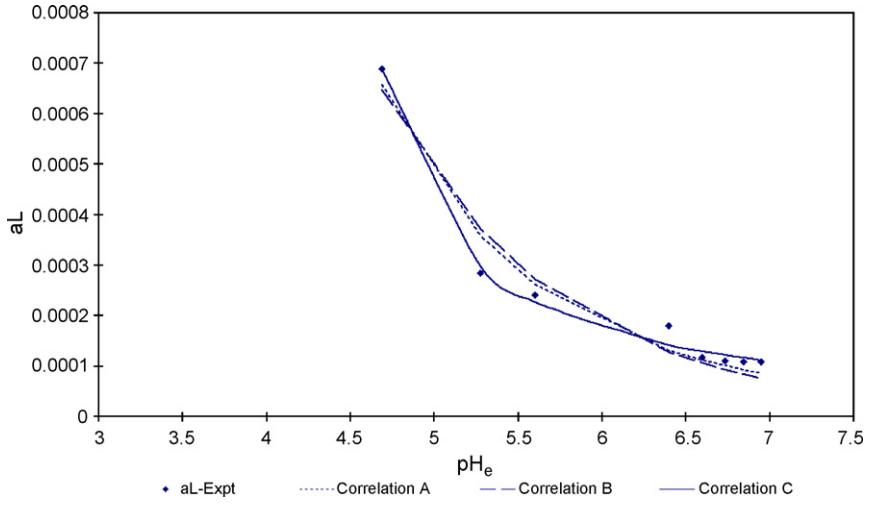


**Fig. 7.** Langmuir isotherm parameter ($a_L$) against equilibrium pH ($pH_e$).

**Table 6**
Summary of correlation parameters on isotherm equations with equilibrium pH, $pH_e$.

| Correlation A | Langmuir | Freundlich | Correlation B | Langmuir | Freundlich | Correlation C | Langmuir | Freundlich |
|---|---|---|---|---|---|---|---|---|
| $\alpha_{K,j}^{(a)}$ | $2.43 \times 10^6$ | $2.42 \times 10^5$ | $\alpha_{K,j}^{(b)}$ | $1.23 \times 10^4$ | $5.77 \times 10^3$ | $\alpha_{K,j}^{(c)}$ | 3.98 | 1.55 |
| $\beta_{K,j}^{(a)}$ | 8.06 | 5.44 | $\beta_{K,j}^{(b)}$ | 1.53 | $9.99 \times 10^{-1}$ | $\beta_{K,j}^{(c)}$ | 2.84 | −66.2 |
| | | | | | | $\gamma_{K,j}^{(c)}$ | 8.65 | $3.69 \times 10^2$ |
| SSE | 0.46 | 44.2 | SSE | 0.22 | 57.7 | SSE | 0.20 | 16.5 |
| $\alpha_{a,j}^{(a)}$ | 2.02 | N/A | $\alpha_{a,j}^{(b)}$ | $5.62 \times 10^{-2}$ | N/A | $\alpha_{a,j}^{(c)}$ | 4.24 | N/A |
| $\beta_{a,j}^{(a)}$ | 5.20 | N/A | $\beta_{a,j}^{(b)}$ | 0.95 | N/A | $\beta_{a,j}^{(c)}$ | $2.91 \times 10^{-6}$ | N/A |
| | | | | | | $\gamma_{K,j}^{(c)}$ | $3.12 \times 10^{-4}$ | N/A |
| SSE | $1.01 \times 10^{-8}$ | N/A | SSE | $8.19 \times 10^{-8}$ | N/A | SSE | $2.32 \times 10^{-9}$ | N/A |
| $m_j$ | N/A | $-4.48 \times 10^{-3}$ | | N/A | $-4.48 \times 10^{-3}$ | | | $-4.48 \times 10^{-3}$ |
| $b_j$ | N/A | 0.66 | | N/A | 0.66 | | | 0.66 |

N/A, not applicable. Correlation A: power relationship; Correlation B: exponent relationship; Correlation C: inverse proportion.

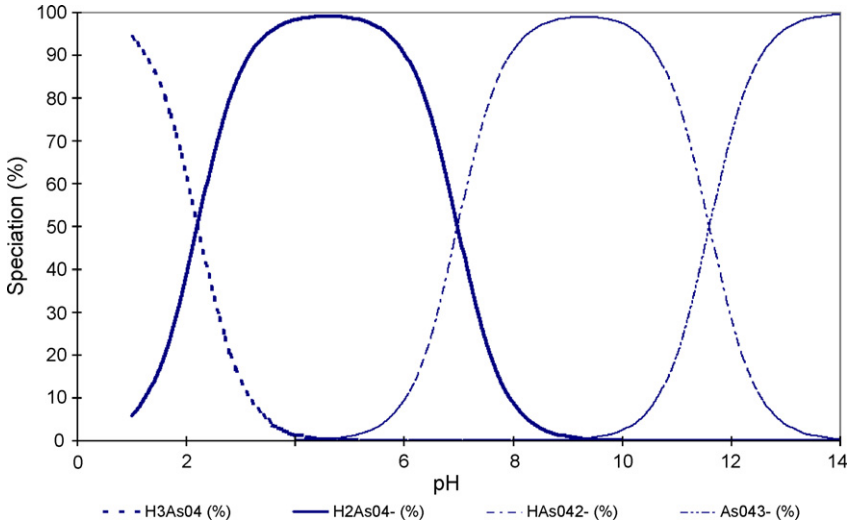


**Fig. 8.** Speciation diagram of arsenate ions with different pH.

(11) and (12)), gives a better fit of correlation to the experimental results.

The free amine groups of chitosan can be protonated under an acidic condition [33]:

$$\text{R-NH}_2 + \text{H}_2\text{O} \Leftrightarrow \text{R-NH}_3^+ + \text{OH}^- \quad (14)$$

The arsenate ions are mainly attached onto the available protonated amine groups. Due to the equilibrium of the protonation of the amine groups (as shown in Eq. (14)), the number of available sorption sites is increased with a decrease of initial pH. Therefore, it is expected to give an inverse proportional relationship between the isotherm parameters and the initial pH.

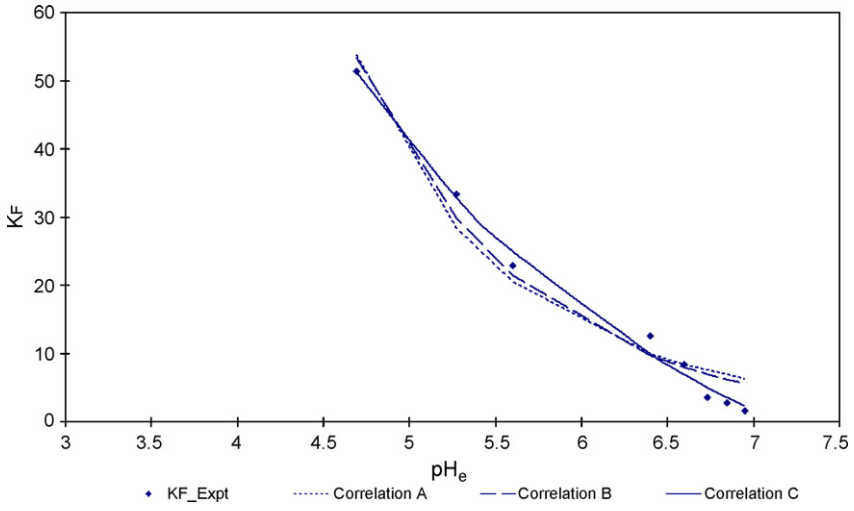


**Fig. 9.** Freundlich isotherm parameter ($K_F$) against equilibrium pH ($pH_e$).

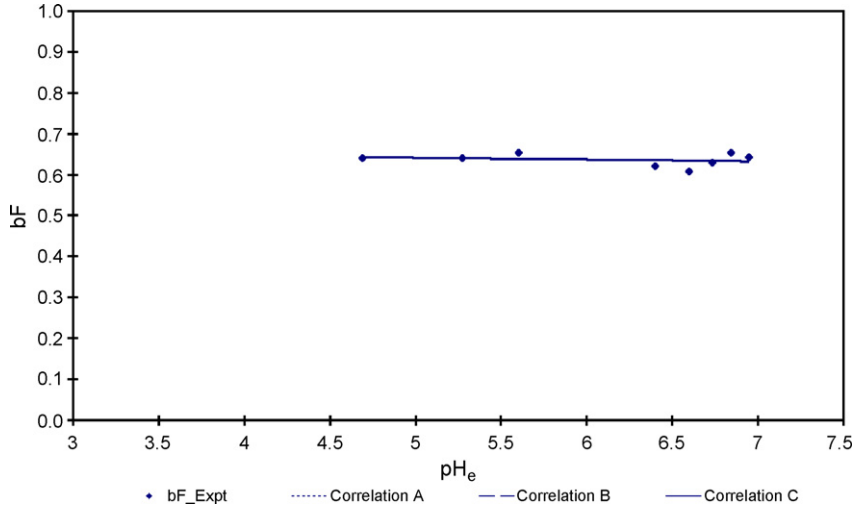


**Fig. 10.** Freundlich isotherm parameter ($b_F$) against equilibrium pH ($pH_e$).

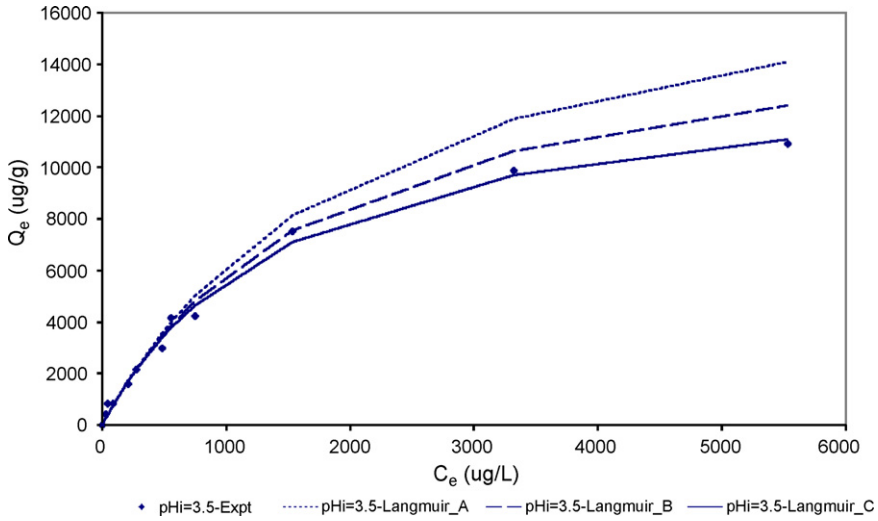


**Fig. 11.** Langmuir isotherm with initial pH ($pH_i$) correlation.

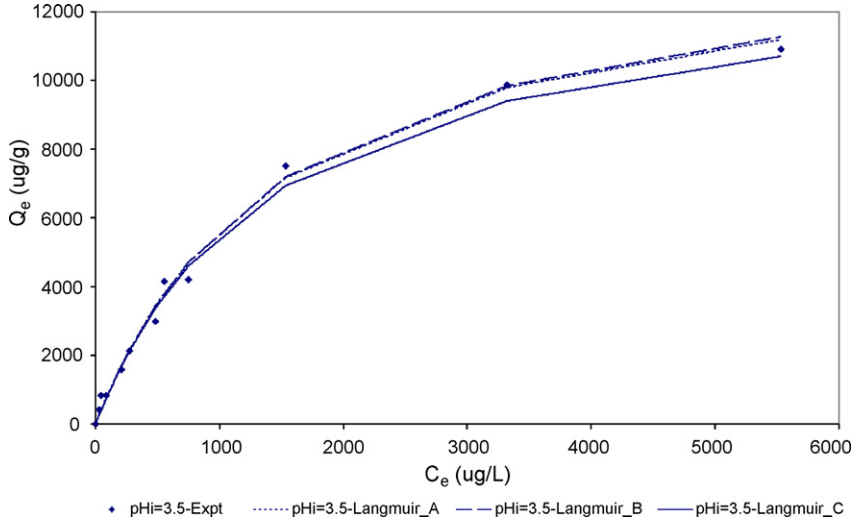


**Fig. 12.** Langmuir isotherm with equilibrium pH ($pH_e$) correlation.

### 3.5. Kinetics of arsenate sorption

The batch kinetic studies were performed for the initial pH ranging from 3.50 to 4.50, as illustrated in Fig. 2. This figure illustrates that there is a rapid drop of liquid-phase concentration within the first 30 min. It can be concluded that there is a rapid sorption of arsenate ion, As(V) within the first 30 min. This rapid drop of liquid-phase concentration leads to a local minimum of the concentration of arsenate ion in the liquid-phase in this sorption system. Due to the mass balance of arsenate ion within the system, there is a local maximum of the concentration of arsenate ion in the solid-phase. After this point of local maximum solid-phase concentration (or minimum liquid-phase concentration), the liquid-phase concentration of arsenate was observed to be increasing. A slow desorption of the As(V) ion gradually occurred. The rate of desorption of arsenate from chitosan increased with the increase of the initial pH from 3.50 to 4.50. The value of the equilibrium pH was determined to be higher than the value of initial pH (by 0.5–1.0 unit of pH). The pH profiles against contact time for the batch kinetic studies with initial pH ranged from 3.50 to 4.50 are shown in Fig. 13. As the capacity of the arsenate ion on chitosan is governed by the protonation reaction of chitosan as shown in Eq. (14) and the dominant speciation of arsenic ions in the system as $H_2AsO_4^-$, an increase of pH leads to a decrease of the protonated groups on chitosan which are available for sorption of arsenate ion and influence the speciation of arsenate ions in the aqueous phase. The speciation change of arsenate ions upon changing pH based on the dissociation constants $pK_a$ of arsenic acid ($H_3AsO_4$) is shown in Fig. 8. As the equilibrium studies and the batch kinetic studies of arsenate and chitosan were performed with the initial pH ranged from 3.50 to 5.50 and the equilibrium pH ranged from 4.00 to 6.95, the dominant arsenate ions is in the form of $H_2AsO_4^-$. It is believed that the removal mechanism of arsenate ions from the aqueous phase might be due to the adsorption of arsenate ions to the protonated amine group on chitosan as expressed by

$$\text{R-NH}_3^+ + \text{H}_2\text{AsO}_4^- \Leftrightarrow \text{R-NH}_3{\bullet}\text{H}_2\text{AsO}_4 \quad (15)$$

Further studies on the interaction between arsenate ions and chitosan upon adsorption may be necessary.

Conventional kinetic models, such as the pseudo-first order and pseudo-second order models, can be used to describe the sorption of arsenate ions and chitosan in the current study [34]. However, the desorption section of the batch kinetic results in the current study cannot be modelled by these two conventional kinetic models. A pseudo-first order reversible model has been developed to describe the sorption and the desorption of the batch kinetic systems of As(V) and chitosan simultaneously.

The rate law for the sorption section can be described by Eq. (16):

$$\frac{dq_t}{dt} = k_{+1}(q_{max} - q_t) \quad (16)$$

The rate law for the desorption section can be represented by Eq. (17):

$$\frac{dq_t}{dt} = -k_{-1}q_t \quad (17)$$

By combining Eqs. (16) and (17), it becomes

$$\frac{dq_t}{dt} = k_{+1}(q_{max} - q_t) - k_{-1}q_t \quad (18)$$

With the initial condition $q_t = 0$ with $t = 0$, $t \to \infty$, $q_t \to q_e$, the solution of Eq. (18) is

$$q_t = \frac{k_{+1}q_{max}}{k_{-1} - k_{+1}}(e^{-k_{+1}t} - 1) - \left(q_e + \frac{k_{+1}q_{max}}{k_{-1} - k_{+1}}\right)(e^{-k_{-1}t} - 1) \quad (19)$$

It is found that the pH value of the aqueous phase increases against time upon contact with chitosan as shown in Fig. 13. A correlation has been developed to account for the variation of pH in the kinetic studies against time. The evolution time of liquid-phase concentration upon changes of pH values can be predicted. The correlation equation of pH value and contact time, $t$, is shown in Eq. (20):

$$\frac{[H^+]_t}{[H^+]_i} = 1 - A(1 - \exp(-at)) \quad (20)$$

The value of "1" represents unity in Eq. (20) for the ratio $([H^+]_t/[H^+]_i)$ of the initial values, that is, at $t = 0$, $[H^+]_t = [H^+]_i$. The term, $A(1 - \exp(-at))$, represents the change of the function with respect to time, compared with the initial values.

The correlation is incorporated with the expression of rate constant in desorption, $k_{-1}$, which describes the change in the rate constant with changing concentration of hydrogen ions, as expressed in Eq. (21):

$$k_{-1} = k'_{-1} \times \frac{1}{[H^+]_t} \quad (21)$$

In this model, the values of the equilibrium solid-phase concentration, $q_e$, were determined from the correlation of the equilibrium isotherm equation with initial pH predicted by our Eqs. (11) and (12). The values of model parameters at different initial pH are

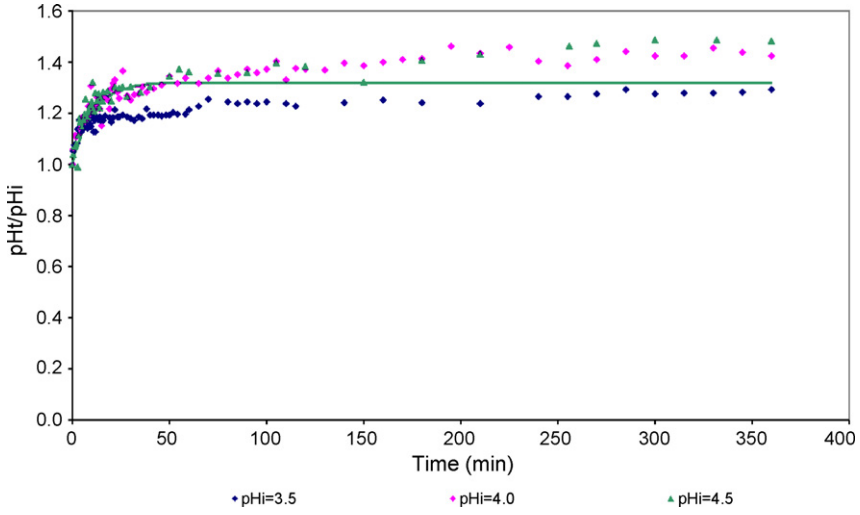


**Fig. 13.** pH profile of chitosan against time in deionised water.

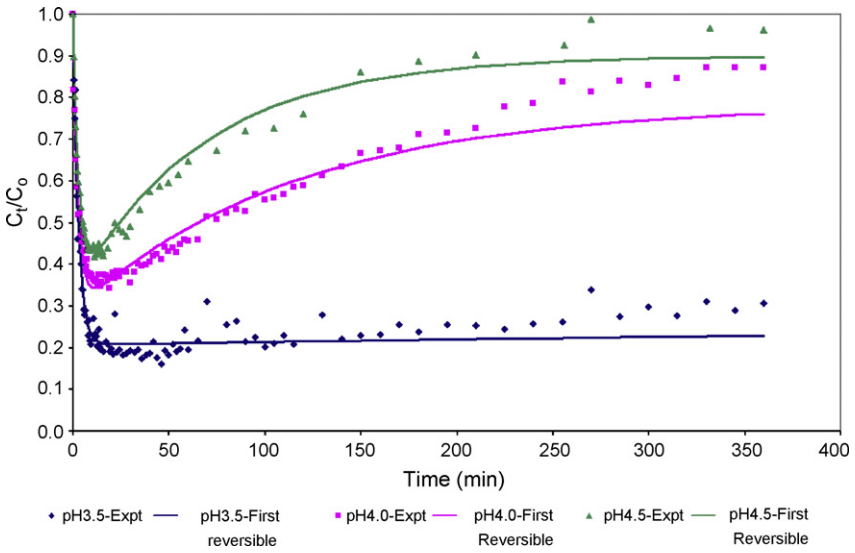


**Fig. 14.** Batch kinetics result with pH correlations ($pH_i$ and $pH_e$).

**Table 7**
Summary of pseudo-first order reversible model parameters.

| $pH_i$ | $pH_e$ | $k_{+1}$ | $k_{-1} \times 10^8$ | $q_{max}$ | $q_e$ | SSE |
|---|---|---|---|---|---|---|
| 3.5 | 4.69 | 3.52E−01 | 4.39 | 3318 | 3125 | 2.17E+06 |
| 4.0 | 6.40 | 3.59E−01 | 4.75 | 3968 | 1236 | 2.85E+06 |
| 4.5 | 6.73 | 3.26E−01 | 4.10 | 3425 | 540 | 1.69E+06 |

shown in Table 7. It can be seen that the rate constants of the sorption step, $k_{+1}$, and the rate constants of the desorption step, $k_{-1}$, are fairly constant for the sorption of As(V) on chitosan at all the initial pH values, namely 3.50, 4.00 and 4.50 and their corresponding final equilibrium $pH_e$ values of 4.69, 6.40 and 6.73.

The kinetics model plots based on Eqs. (11), (12) and (19)–(21) are represented by the solid lines in Fig. 14. The correlation of the experimental concentration decay data using the model equations is very good even at small time values where the sorption reaction is very rapid. The time dependent maximum arsenate adsorption capacity is accurately predicted by the novel kinetic equation (19) and this optimum capacity value is followed by an accurate desorption concentration profile.

## 4. Conclusion

- The sorption ability of arsenate ions on chitosan with different initial pH condition has been studied.
- Three empirical correlation methods have been developed to correlate the effect of initial pH and equilibrium pH into general equilibrium equation models. The performance of the modified equilibrium equation models is similar to that of the original equilibrium equation models. The isotherm parameters in Langmuir and Freundlich models are able to predicted accurately from the equilibrium pH by correlation C in Eqs. (11) and (12). The adsorption capacity of arsenate on chitosan can be determined based on the value of $K_L/a_L$ in Langmuir isotherm.
- A novel pseudo-first order reversible model, incorporating the effect of changing pH profile throughout the adsorption and desorption cycle, has been newly developed to describe the sorption and the desorption in the batch kinetic systems of As(V) and chitosan simultaneously. The pH value of the adsorption and desorption reaction of arsenate and chitosan can be predicted from the pH against time profile. Furthermore, the rate constant of the desorption step, $k_{-1}$, can be predicted from the correlation with the concentration of hydrogen ions in the system, which can be expressed in terms of the pH value.

## Acknowledgement

The authors (K.C.M., Kwok and V.K.C. Lee) would like to thank Hong Kong RGC for the provision of support throughout this research study.

## References

[1] S.L. Chen, S.R. Dzeng, M.H. Yang, K.H. Chiu, G.M. Shieh, C.M. Wai, Arsenic species in groundwaters of the Blackfoot Disease Area, Taiwan, Environ. Sci. Technol. 28 (1994) 877–881.
[2] M. Berg, H.C. Tran, T.C. Nguyen, H.V. Pham, R. Schertenleib, W. Giger, Arsenic contamination of groundwater and drinking water in Vietnam: a human health threat, Environ. Sci. Technol. 35 (2001) 2621–2626.
[3] J. Reid, Arsenic occurrence, USEPA Seeks Clearer Picture 86 (1994) 44–51.
[4] J.M. Desesso, C.F. Jacobson, A.R. Scialli, C.H. Farr, J.F. Holson, An assessment of the developmental toxicity of inorganic arsenic, Reprod. Toxicol. 12 (1998) 385–433.
[5] European Union, European Commission Directive 98/83/Ec, Related with drinking water quality intended for human consumption, (1998).
[6] USEPA, Integrated Risk Information System. http://www.epa.gov/iris/.
[7] D. Caussy, Case studies of the impact of understanding bioavailability: arsenic, Ecotox. Environ. Safe. 56 (2003) 164–173.
[8] J.G. Hering, P.Y. Chen, J.A. Wilkie, M. Elimelech, S. Liang, Arsenic removal by ferric chloride, J. Am. Water Work Assoc. 88 (1996) 155–167.
[9] S.K. Gupta, K.Y. Chen, Arsenic removal by adsorption, Res. J. Water Pollut. C 50 (1978).
[10] D.A. Clifford, G.L. Ghurye, A.R. Tripp, As removal using ion exchange with spent brine recycling, J. Am. Water Work Assoc. 95 (2003) 119–130.
[11] M.J. Scott, J.J. Morgan, Reactions at oxide surfaces. 1. Oxidation of As(III) by synthetic birnessite, Environ. Sci. Technol. 29 (1995) 1898–1905.
[12] T.S. Singh, K.K. Pant, Equilibrium, kinetics and thermodynamic studies for adsorption of As(III) on activated alumina, Sep. Purif. Technol. 36 (2004) 139–147.
[13] W.R. Richmond, M. Loan, J. Morton, G.M. Parkinson, Arsenic removal from aqueous solution via ferrihydrite crystallization control, Environ. Sci. Technol. 38 (2004) 2368–2372.
[14] S. Fendorf, M.J. Eick, P. Grossl, D.L. Sparks, Arsenate and chromate retention mechanisms on goethite. 1. Surface structure, Environ. Sci. Technol. 31 (1997) 315–320.
[15] D.B. Singh, G. Prasad, D.C. Rupainwar, Adsorption technique for the treatment of As(V)-rich effluents, Colloid Surf. A-Physicochem. Eng. Asp. 111 (1996) 49–56.
[16] S.P. Kamble, S. Jagtap, N.K. Labhsetwar, D. Thakare, S. Godfrey, S. Devotta, S.S. Rayalu, Defluoridation of drinking water using chitin, chitosan and lanthanum-modified chitosan, Chem. Eng. J. 129 (2007) 173–180.

[17] C. Gerente, V.K.C. Lee, P. Le Cloirec, G. McKay, Application of chitosan for the removal of metals from wastewaters by adsorption—mechanisms and models review, Crit. Rev. Environ. Sci. Technol. 37 (2007) 41–127.
[18] I. Langmuir, The constitution and fundamental properties of solids and liquids. I. Solids, J. Am. Chem. Soc. 38 (1916) 2221–2295.
[19] H. Freundlich, Uber die adsorption in losungen, Z. Physik. Chem. 57 (1906) 385–471.
[20] A. Shafaei, F.Z. Ashtiani, T. Kaghazchi, Equilibrium studies of the sorption of Hg(II) ions onto chitosan, Chem. Eng. J. 133 (2007) 311–316.
[21] W. Zhang, P. Singh, E. Paling, S. Delides, Arsenic removal from contaminated water by natural iron ores, Miner. Eng. 17 (2004) 517–524.
[22] A.C.Q. Ladeira, V.S.T. Ciminelli, Adsorption and desorption of arsenic on an oxisol and its constituents, Water Res. 38 (2004) 2087–2094.
[23] S.S. Tripathy, A.M. Raichur, Enhanced adsorption capacity of activated alumina by impregnation with alum for removal of As(V) from water, Chem. Eng. J. 138 (2008) 179–186.
[24] H. Genc-Fuhrman, J.C. Tjell, D. McConchie, Adsorption of arsenic from water using activated neutralized red mud, Environ. Sci. Technol. 38 (2004) 2428–2434.
[25] C.K. Lee, K.S. Low, S.C. Liew, C.S. Choo, Removal of arsenic(V) from aqueous solution by quaternized rice husk, Environ. Technol. 20 (1999) 971–978.
[26] G.N. Manju, C. Raji, T.S. Anirudhan, Evaluation of coconut husk carbon for the removal of arsenic from water, Water Res. 32 (1998) 3062–3070.
[27] M.X. Loukidou, K.A. Matis, A.I. Zouboulis, M. Liakopoulou-Kyriakidou, Removal of As(V) from wastewaters by chemically modified fungal biomass, Water Res. 37 (2003) 4544–4552.
[28] H. Genc-Fuhrman, J.C. Tjell, D. McConchie, Increasing the arsenate adsorption capacity of neutralized red mud (bauxsol), J. Colloid Interf. Sci. 271 (2004) 313–320.
[29] E.A. Deliyanni, D.N. Bakoyannakis, A.I. Zouboulis, E. Peleka, Removal of arsenic and cadmium by akaganeite fixed-beds, Sep. Sci. Technol. 38 (2003) 3967–3981.
[30] L. Lorenzen, J.S.J. Vandeventer, W.M. Landi, Factors affecting the mechanism of the adsorption of arsenic species on activated carbon, Miner. Eng. 8 (1995) 557–569.
[31] C.A. Impellitteri, K.G. Scheckel, J.A. Ryan, Sorption of arsenate and arsenite on $RuO_2$ center dot Xh(2)O: a spectroscopic and macroscopic study, Environ. Sci. Technol. 37 (2003) 2936–2940.
[32] K.P. Raven, A. Jain, R.H. Loeppert, Arsenite and arsenate adsorption on ferrihydrite: kinetics, equilibrium, and adsorption envelopes, Environ. Sci. Technol. 32 (1998) 344–349.
[33] Q.Z. Wang, X.G. Chen, N. Liu, S.X. Wang, C.S. Liu, X.H. Meng, C.G. Liu, Protonation constants of chitosan with different molecular weight and degree of deacetylation, Carbohydr. Polym. 65 (2006) 194–201.
[34] Y.S. Ho, G. McKay, Pseudo-second order model for sorption processes, Proc. Biochem. 34 (1999) 451–465.
[35] L. Dambies, E. Guibal, A. Roze, Arsenic(V) sorption on molybdate-impregnated chitosan beads, Colloid Surf. A-Physicochem. Eng. Asp. 170 (2000) 19–31.
[36] K.H. Goh, T.T. Lim, Geochemistry of inorganic arsenic and selenium in a tropical soil: effect of reaction time, pH, and competitive anions on arsenic and selenium adsorption, Chemosphere 55 (2004) 849–859.
[37] R. Weerasooriya, H.J. Tobschall, H.K.D.K. Wijesekara, E.K.I.A.U.K. Arachchige, K.A.S. Pathirathne, On the mechanistic modeling of As(III) adsorption on gibbsite, Chemosphere 51 (2003) 1001–1013.